Chapter 4

Generation, Evolution, and Characterization of Turbulence Coherent Structures

Zambri Harun and Eslam Reda Lotfy

Additional information is available at the end of the chapter

http://dx.doi.org/10.5772/intechopen.76854

Abstract

Turbulence stands as one of the most complicated and attractive physical phenomena. The accumulated knowledge has shown turbulent flow to be composed of islands of vortices and uniform-momentum regions, which are coherent in both time and space. Research has been concentrated on these structures, their generation, evolution, and interaction with the mean flow. Different theories and conceptual models were proposed with the aim of controlling the boundary layer flow and improving numerical simulations. Here, we review the different classes of turbulence coherent structures and the presumable generation mechanisms for each. The conceptual models describing the generation of turbulence coherent structures are generally classified under two categories, namely, the bottom-up mechanisms and the top-down mechanisms. The first assumes turbulence to be generated near the surface by some sort of instabilities, whereas the second assigns an active role to the large outer layer structures, perhaps the turbulent bulges. Both categories of models coexist in the flow with the first dominating turbulence generation at low Reynolds number and the second at high Reynolds number, such as the case in the atmospheric boundary layer.

Keywords: boundary layer, turbulence, coherent structures, generation, ejection, sweep

1. Introduction

Turbulent flow is the most common flow in industrial applications and atmospheric phenomena. The random motion inherent in the flow contributes the largest share of fluid mixing and interaction with solid surfaces (e.g. friction, heating, and pollutant dispersion). Natural ventilation in modern cities, flow-induced vibrations of large civil structures, performance of windmills, etc. keep the topic ever interesting. Hundreds of researches have been devoted to the subject aiming at characterizing this randomness. The main objectives are (1) to set an

exact solution (or at least a mathematical model) to the turbulent flow problem and (2) to control it, for example, modify vortices and thereby reduce the drag on surfaces.

The random appearance of turbulent flow is violated by many well-established evidences. For instance, compared to a random signal, the turbulent velocity signal displays non-zero trends in both the energy spectrum (**Figure 1**) and autocorrelation (**Figure 2**) analyses. These examples, among many others, reveal the existence of organized motions within the irregular background. These organized motions are termed turbulence coherent structures (TCSs). Thus, TCSs are either vortices or uniform-momentum regions within the turbulent flow; these structures maintain their coherence over remarkable extents in time and space. The TCSs play a prominent role in the transport and mixing processes within the turbulent flow.

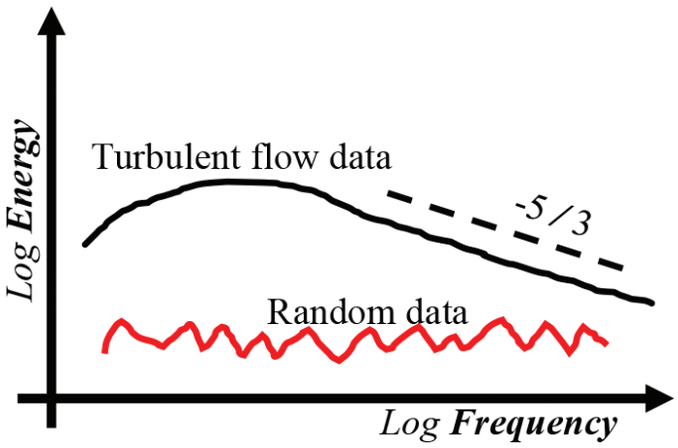

Figure 1. Energy spectrum of turbulent flow compared to a random signal.

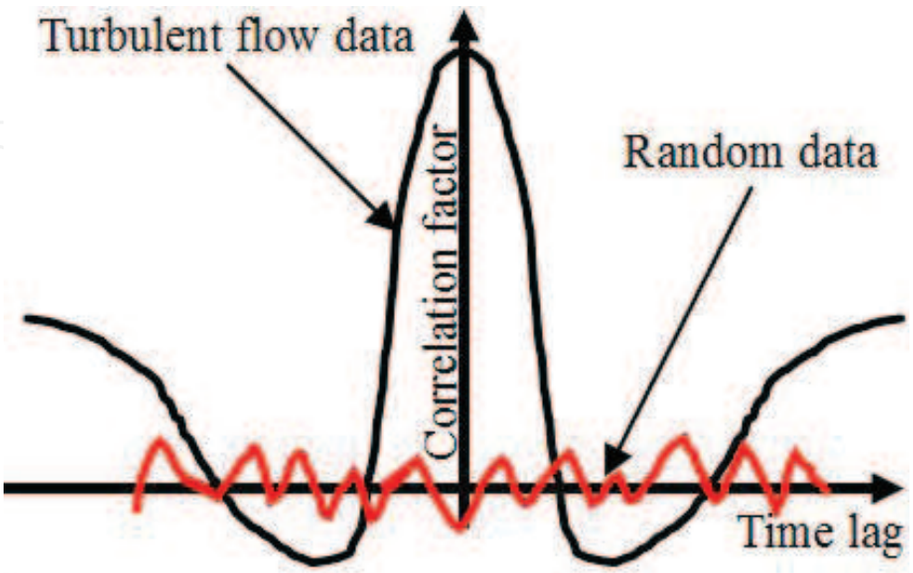

Figure 2. Autocorrelation function of turbulent flow compared to a random signal.

http://dx.doi.org/10.5772/intechopen.76854

Accordingly, few friction-reduction schemes target manipulating the TCSs. Furthermore, few researches attribute large parts of the loading on windmills to the TCSs. It follows that the understanding of TCSs is inevitable in solving and controlling turbulent flows.

In this chapter, we focus on the basic kinds of TCSs and their presumable generation mechanisms. We start with the *hairpin vortex*, which is the elementary building block of TCSs. We characterize the hairpin vortex and detail its popular *bursting* theory of generation. Afterwards, we discuss the *vortex packets* and *superstructures*, which form the turbulent/non-turbulent interface bulges and contribute around half the turbulent kinetic energy and turbulent transport. Finally, we review the theories of TCS generation in high-Reynolds number flows.

2. The hairpin vortex

The first conceptual model for TCSs was proposed by Theodorsen [1]. From his observations, he noticed the turbulence vortex to take a *hairpin* or *horseshoe* shape with the legs aligned streamwise and the head located downstream and curved up, **Figure 3**. Theodorsen applied a vorticity-based version of Navier-Stokes equations to the proposed model vortex. He hypothesized the head to be inclined at an angle 45° to the mean flow direction since it subjects the hairpin to the maximum stretching from the mean flow and hence achieves the maximum turbulence production. The legs (streamwise vortices) induce upward flow on the head, which causes it to be lifted up. The vortex is then subjected to stretching by the mean flow since the head lies in a higher-velocity region than the legs (shear effect), see **Figure 4**. This shear causes the vortex to extend in length and compress in diameter. Consequently, the vorticity intensifies, that is, rotation becomes faster and hence more lifting force is generated and the head moves up further. This sequence is resisted only by the shear stress which, although lengthening the vortex, exerts a restoring moment on the head to return it to the zero-shear horizontal position. The inclination angle of the vortex will depend on the balance between the two conflicting effects. The hairpin vortex model was first verified experimentally by Head and Bandyopadhyay [2] through a smoke visualization experiment. They measured the

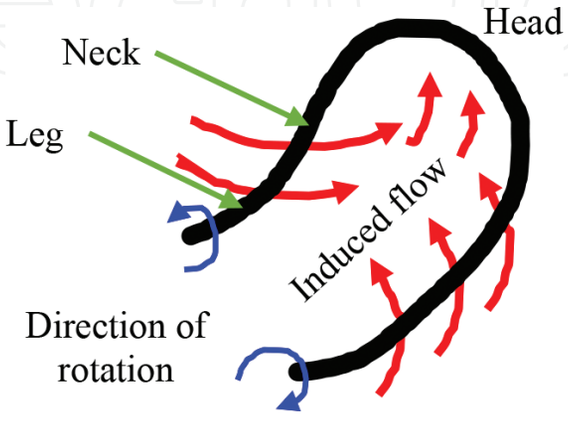

Figure 3. Illustration of the hairpin vortex model; vortex head lifting by induction from the legs.

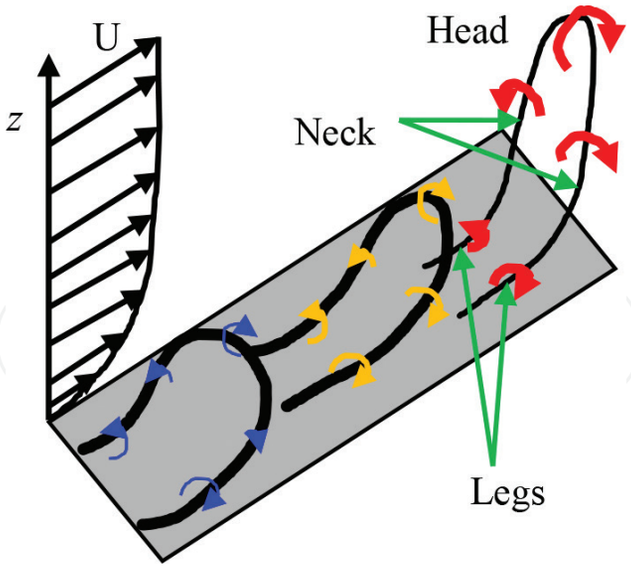

Figure 4. Hairpin vortex stretching.

angle and found it to fall well between 40 and 50°. As justified by Head and Bandyopadhyay, the angle of principal stress in the pure shear flow is 45°. Brief reviews of Theodorsen's paper are found in [2–4].

Long before the first documented visualization of the hairpin vortices, Theodorsen's model was confirmed, partly, by the correlation analysis of Townsend [5] and Grant [6] which was developed in [7]. Townsend depicted the dominant TCSs as randomly located couples of counter-rotating vortices aligned in the streamwise direction. These vortices (eddies) are of cone-like structure with the vertex upstream and the base downstream. An eddy size scales with its distance from the wall; hence his model is named the *attached eddy* model. The attached eddies can be thought of as headless hairpin vortices. In addition to Townsend, Willmarth, and Tu [8] conducted pressure-velocity correlation analysis that demonstrated the turbulence coherent structure as a transverse row of inclined triangular tubular vortices.

The symmetric structure of the hairpin vortex is the exception rather than the rule [3, 9–13]. The turbulence-inherent perturbations of the background flow cause the generated hairpin to be born distorted, for example, one-legged. Zhou et al. [14] examined the conditions to synthesize hairpin vortices by utilizing direct numerical simulation (DNS). They found the asymmetric hairpins to form more readily in rapid succession and at smaller streamwise separation. In the same article, Zhou et al. explained how the induction of the hairpin legs could cause the head to deform into an Ω-shaped structure. Thus, the transverse vortex can exist in many forms; cane, hairpin, horseshoe, or Ω -shaped vortices and deformed versions.

With or without the legs being attached to the wall, a hairpin vortex persistently rises across the boundary layer. The vortex envelope expands in the wall-normal and spanwise directions. The vortex core enlarges and weakens due to shear relaxation in the outer layer. Along the way up, hairpin-hairpin merging occurs to form larger and stronger vortices [15]. The hairpins align streamwise in groups (packets) to form the bulges at the edge of the turbulent boundary layer [2, 16–18], see **Figure 5**. Ultimately, under excessive stretching, the hairpin legs get very close

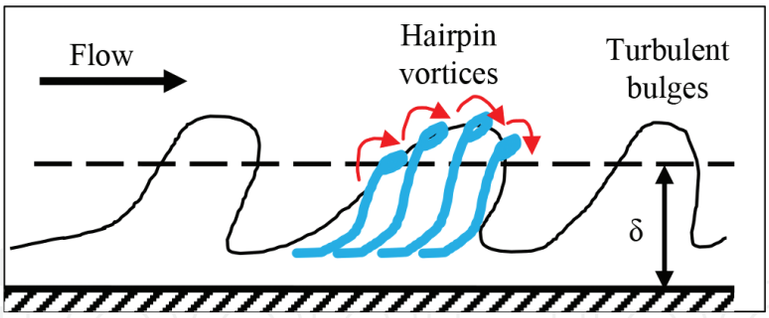

Figure 5. Hairpin vortices may reach the end of the TBL to compose the turbulent/non-turbulent interface bulges.

and cancel each other i.e. the vortex dies [18]. However, the vortex dies anyway after a while by viscous diffusion. The debris from the dead eddies is convected away from the wall and undergoes stretching and distortion by live eddies to form isotropic fine-scale eddies surrounding the attached eddies [15]. Lozano-Durán and Jiménez [19] performed a DNS to inspect the evolution of coherent structures. They argue the tendency of eddies to remain small and die shortly; few eddies only attach to the wall and expand self-similarly across the logarithmic layer. These hold-on for lifetimes, which are proportional to their distances from the wall. These eddies are responsible for the vast majority of momentum transport. The hairpin vortices transport the low-momentum fluid from the wall layer to the outer layer. The hairpins are the main elements responsible also for vortex regeneration and hence the self-sustenance of flow turbulence [20, 21].

3. From eddies to turbulence

The coordinate system is defined by x, y, and z as the streamwise, spanwise, and wall-normal directions and the velocity components are given by u, v, and w, respectively. The time-mean and fluctuating components are referred to by capital letters and (′) signs. The stirring effect of the vortices is illustrated in **Figure 6**. The rotation of the hairpin vortices, either the head or legs, disturbs the fluid in two ways. The low-speed fluid ($-u'$) from the bottom layers is pumped upward ($+w'$), an event named *second-quadrant* or Q2 event, whereas the high-speed fluid ($+u'$) from the top layers is pumped downward ($-w'$), an event named *fourth-quadrant* or Q4 event. Experiments held by [22] have proven the Reynolds' turbulent stresses $\overline{u'w'}$ to be formed up of

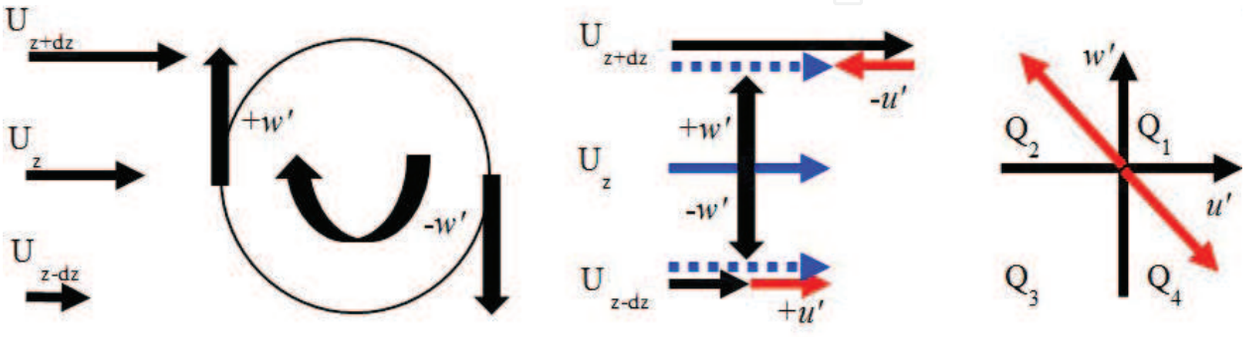

Figure 6. Q2 and Q4 events.

mainly Q2 and Q4 events. That means, the Q2 and Q4 fluctuations are more probable than Q1 and Q3 ones [3]. The turbulent kinetic energy is defined as $k = \frac{1}{2}(\overline{u'^2 + v'^2 + w'^2})$. The literature, especially of numerical analysis, defines the production of the turbulent kinetic energy as $\overline{u'w'}\frac{\partial U}{\partial z}$ [23]. Hence, it can be said that hairpin vortices by their stirring action are the *turbulence producers* i.e. they cause the fluctuations read by the hotwire probe or pressure transducer. Some researchers like to make a shortcut by identifying vortex generation as *turbulence production*.

4. Generation of the hairpin vortex

The generation of hairpin vortices is attributed *mainly* to what is called the *bursting* process [3, 10], which occurs in the buffer layer. Before proceeding with the bursting process, it is better to introduce the *low-speed streak*, which is the key element in the bursting process. The low-speed streaks are long, narrow, uniform-momentum regions aligned quasi-streamwise, see **Figure 7**. They exist exclusively in the inner layer (below z^+~10) and move downstream at speeds lower than the mean flow speed (where $z^+ = \frac{u^* z}{\nu}$, ν is the kinematic viscosity, and u^* is the friction velocity). The streaks were first observed by Francis Hama [24] and concurrently by Ferrell et al. [25] in tube flow by injecting dye through a slot in the wall in the first experiment and by flushing a flow of colored water by a clear fluid in the second experiment.

The streaks can extend in length to 1000 viscous (wall) units [26, 27] (one viscous unit $= \frac{u^*}{\nu}$) and in width to 20 viscous units [28]. The transverse spacing between streaks depends on the turbulent Reynolds number, $Re_\tau = \frac{\delta u^*}{\nu}$, or momentum-thickness Reynolds numbers, $Re_\theta = \frac{\theta U_\infty}{\nu}$, [29] (where θ is the momentum thickness). The streak transverse spacing is equal to $\lambda_y^+ = 100$ at $Re_\theta = 2000$ [30] and widens to $\lambda_y^+ = 200$ at $Re_\theta = 40{,}000$ [8, 31]. Nevertheless, a later study by Smith and Metzler [32] for $740 < Re_\theta < 5830$ suggested the low-speed streaks to have an invariant spacing of $\lambda_y^+ = 100$. This value was found to provide the maximum energy amplification of a perturbation in turbulent flow [33–35]. It is worth noting that a flow domain of spanwise extent less than $\lambda_y^+ = 100$ cannot sustain turbulence [36].

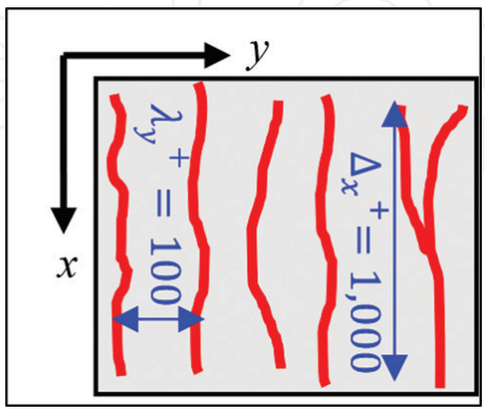

Figure 7. Low-speed streaks.

http://dx.doi.org/10.5772/intechopen.76854

5. The bursting process

The bursting process as described by Kline et al. [37] and Kim et al. [29], with updates from later observations, passes through three stages:

1. *Streak-lifting*: The streak moves downstream and migrates gradually from the wall. The streak becomes thinner as it drifts outward. After a certain critical distance, the streak is lifted up rapidly away from the wall. This streak transports the low-momentum fluid near the wall to the upper layers, which causes an inflection in the streamwise instantaneous velocity profile. A spanwise *shear layer* is formed atop the streak upstream or downstream the crest. The shear layer (*vorticity layer*) is a circulating area of fluid of elliptic or generally non-circular shape. The shear layer rolls up in a circular form to generate a spanwise vortex (circular shear layer). The vortex is then stretched and lifted by the mean shear to form a streamwise and/or a hairpin vortex. Thus, streamwise and/or spanwise vortices propagate downstream the inflection point.
2. *Oscillation*: When the streak reaches a height of $z+ = 8-12$, it starts to oscillate. The oscillations are three-dimensional, that is, can be seen in both $x-z$ and $x-y$ planes and tend to be regular and organized.
3. *Break-up*: After a certain number of oscillations (3–10) the motion turns to be random and violent. This ends up with the streak broken-up and disappeared.

It follows then a quiescent period before the cycle is repeated. An illustration of the bursting process is shown in **Figure 8**. The oscillations of the streak are actually due to the formation and stretching of the born vortices. The concluding violent motion is imputed to the vortex stretching under the combined effect of turbulent background and successive-ascent through higher-faster-layers [38]. Smith and Metzler [32] discovered that the streak does not break down after the bursting process. It rather persists owing to the reinforcement by the legs of the new hairpins.

Corino and Brodkey [39] complemented the picture with a *sweep* at the onset of the burst sequence and multiple *ejections* of low-momentum fluid followed by a *sweep* at the end of process. An ejection is a Q2 event, while a sweep is a Q4 event. The sweep at the onset of the burst may be responsible for lifting the streak. As elucidated by Grass [40], the sweep (inrush) stream triggers the bursting process, while the ejection stream is a consequence of the bursting process and can extend across the entire boundary layer. On the other hand, Nakagawa and Nezu [41] and Smith [42] suggested the final ejections and sweep to be invoked by the generated hairpin vortices. The inward side of the vortex entrains low-momentum fluid from the streak and pumps it upward. The vortex navigation over the streak appears like multiple rapid ejections, whereas the outboard side entrains high-momentum fluid from the upper layers and pumps it toward the lateral extremes of the streak. Since the vortex is already inclined to the flow direction, the ejection and sweep appear as Q2 and Q4 events, see **Figure 9**.

Smith [42] considered each burst to be responsible for generating 2–5 vortices. Kline et al. [37] also estimated the frequency of bursts and found it to match with the dominant frequency

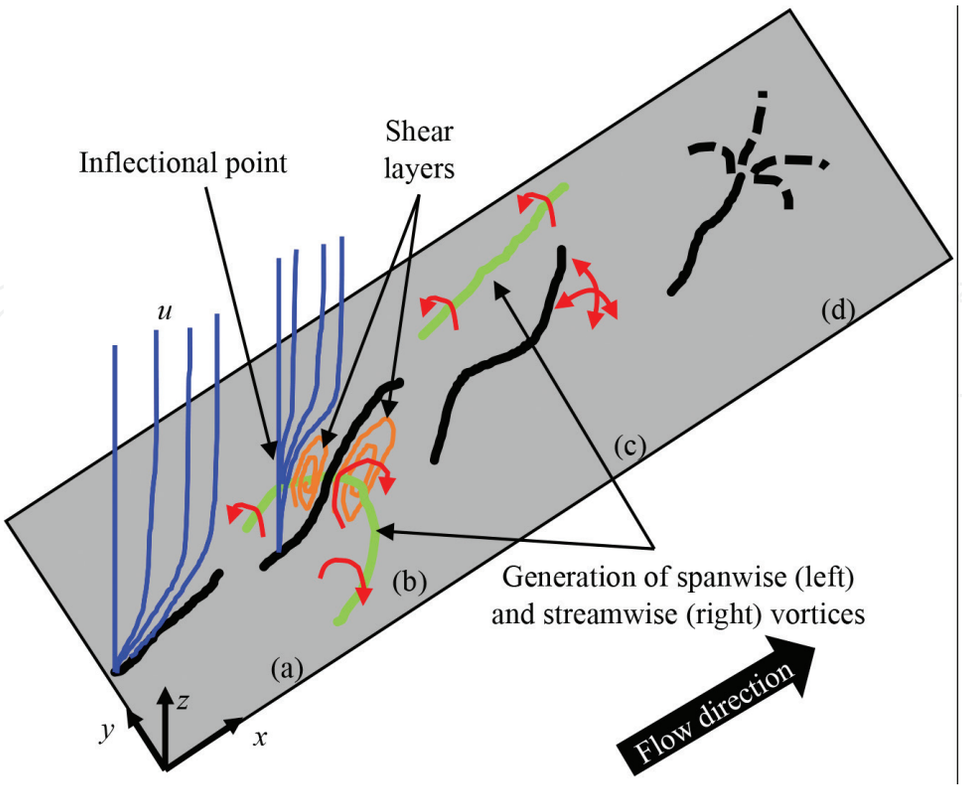

Figure 8. The bursting process as described by Kim et al. [29]. (a) Low-speed streak moving downstream and gradually lifting away from the wall. (b) Streak-lifting: the streak is lifted rapidly. (c) Oscillation: the streak starts an organized 3-D oscillation. (d) Break-up: random, violent oscillations that end with the streak broken up into small motions.

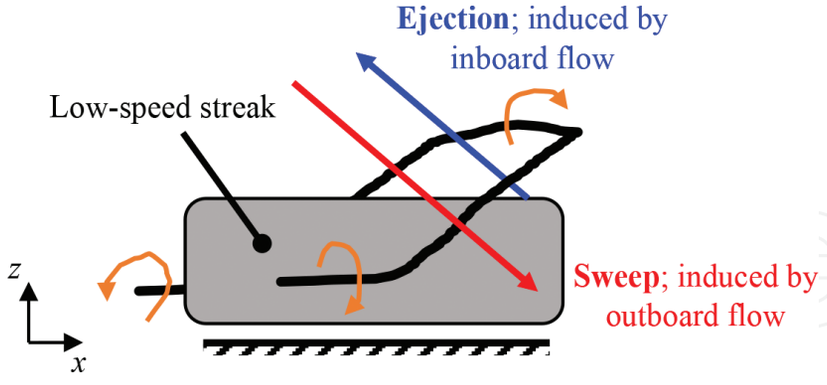

Figure 9. Ejection and sweep events caused by a hairpin vortex.

in the wall-pressure spectrum analysis held by Black [43]. Kim et al. [29] found that most/all occurrences of turbulent stresses ($-\overline{u'w'}$) take place not only in the near-wall region but entirely during the bursting process, which opts the bursting to be the main turbulence producer. This harmonizes with the early predictions of Runstadler et al. [44]. Kline et al. [37] anticipated the death of turbulence (*flow relaminarization*) when suppressing the bursting process and fetched many examples in this context:

- Relaminarizing turbulent boundary layer flow by applying a favorable pressure gradient; the pressure gradient hinders the lift-up process (a conclusion of the same paper [37] and other later, more comprehensive researches [45, 46]).
- Relaminarizing turbulent flow in a tube by rotating the tube about its axis; the centrifugal force affixes the streaks to the tube wall [47].
- Relaminarizing turbulent flow in a 2-D channel by rotating the channel about an axis fixed at one of the narrow walls and perpendicular to the mean flow direction; the Coriolis force suppresses turbulence at one wall and strengthens it at the other wall [48].

6. Streak generation

The streaks are created by streamwise vortices occupying the wall region [28, 49, 50]. Each streamwise vortex pumps the fast fluid from upper layers in one y direction and the slow fluid from wall-vicinity in the second direction. This action packs a body of high streamwise velocity at one side of the vortex and another of low streamwise velocity at the other side. These are termed the high-speed and low-speed streaks, see **Figure 10**.

For dye injected (or hydrogen bubbles generated) near the wall, the pumping action of the vortices accumulates the dye together with the wall-adjacent fluid in the low-speed streak. This is why the low-speed streaks appear in flow visualization experiments. It has been recorded that a streak can exist by its own [51], that is, the streamwise vortices form the streak and leave it behind. The streamwise vortices can be the legs of hairpin vortices. This means the streaks generate the hairpin vortices which in turn generate new streaks. This closes the turbulence self-sustenance cycle. The streak-hairpin-streamwise vortex mechanism is only one presumable mechanism for turbulence generation/maintenance among few others.

Robinson [10] and Schwartz [52] believed the low-speed streak to be lifted up or kinked by flow-induction from a streamwise vortex. Offen and Kline [53, 54] and Smith [42] have a somehow longer explanation. The vortical remnant from an upstream burst forms a traveling

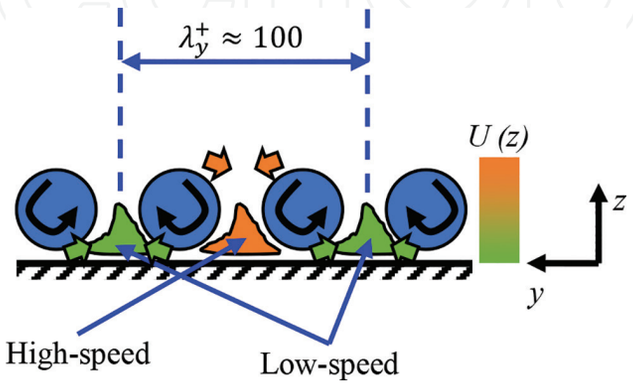

Figure 10. High- and low-speed streak generation by streamwise counter-rotating vortices.

pressure disturbance (instability). This traveling disturbance if passed over a low-speed streak impresses a local adverse pressure gradient upon a portion of it. This decelerates a part of the streak and hence lifts it up.

7. Generation of streamwise vortices

The streamwise, quasi-streamwise, vortices or rolls are the main turbulence producers in the viscous sublayer and responsible for low-speed streak formation. They are generated by different mechanisms:

1. They can be simply the legs of hairpin vortices. The legs of a hairpin vortex are quasi-streamwise and are usually attached to the wall i.e. lie in the sublayer. They range in length between 100 and 200 wall units [14]. There are two theories to interpret how these relatively short legs can produce the long streaks (Δ_x^+~1,000). First, they sweep downstream along the wall, pack the streak and leave it behind in the long trails [55]. Second, many legs coalesce together and create the streak [21, 42, 56].

2. The streamwise vortices can be regenerated by other streamwise vortices [4, 14, 57, 58]. The shear (velocity gradient, $\frac{\partial U}{\partial z}$) causes the quasi-streamwise vortices to be stretched and lifted, that is, the upstream side is attached and the downstream side is detached from the wall (~9 ° inclination angle). Besides, the flow induced by other neighboring vortices tilts them in the spanwise direction (±4 °). The wall-normal detachment motion and spanwise tilt motion provoke high vorticity in the wall-normal direction. This wall-normal vorticity is then affected by the shear that stretches it and turns it in the streamwise direction. A child vortex is then born on the downwash side (flow toward the wall) at either the upstream or the downstream ends of the parent vortex. The direction of rotation of the child vortex is opposite to that of the parent vortex. The flow induced by the parent tilts the child in spanwise direction. The legs of a hairpin vortex can produce two pairs of streamwise vortices, inboard and outboard the hairpin [59]. Finally, we get a corrugated line of quasi-streamwise vortices.

3. The streamwise vortices can be generated during the bursting process [60]. Although the interaction between the low-speed streak and the mean flow produces a spanwise shear (vorticity) layer, this can turn in the streamwise direction to form a streamwise vortex. Depending on the presence of the streamwise vortex that lifts the streak, different types of vortices can be generated. If one lifting streamwise vortex is present at one side of the streak, the new vortex extends over it downstream such that the direction of rotation of the new vortex is opposing the old one, while if no streamwise vortices are present beside the streak, then the new vortex evolves in an arch vortex, see **Figure 11**.

4. The streamwise vortices, and even the spanwise vortices, can be produced by some low-speed streak *instability* [10, 50, 55, 61, 62]. An instability (waviness) in the spanwise direction can be excited by the asymmetric flanking-vortices. The waviness generates a streamwise vorticity layer. Once the waviness grows enough, it produces a strong velocity gradient in the streamwise direction, $\frac{\partial u}{\partial x}$. This gradient is responsible for stretching the aforementioned layer and collapsing (compressing) it into a streamwise vortex (circular vorticity

layer). Schoppa and Hussain [61] proposed three possible processes for vortex generation by streak instability—namely Process A: regeneration within gaps between consequent vortices; Process B: regeneration from an existing spanwise (arch) vortex, whose spanwise profile, excites streak instability to produce a pair of new streamwise vortices; and Process C: regeneration at trailing ends of low-speed streaks. Since the spawned vortices travel faster than the streak, they totally advect the streak leaving it behind and a new set of vortices are spawned.

5. Finally, streamwise vortices may generate from existing streamwise vorticity layers [63]. These vorticity layers were observed to evidence near the edge of the viscous sublayer. One layer tends to roll up into a compact streamwise core either due to the mutual induction with its image vorticity layer [50, 64] or by ejection from a parent, opposite signed, vortex [65]. The two mechanisms are illustrated in **Figures 12** and **13**, respectively.

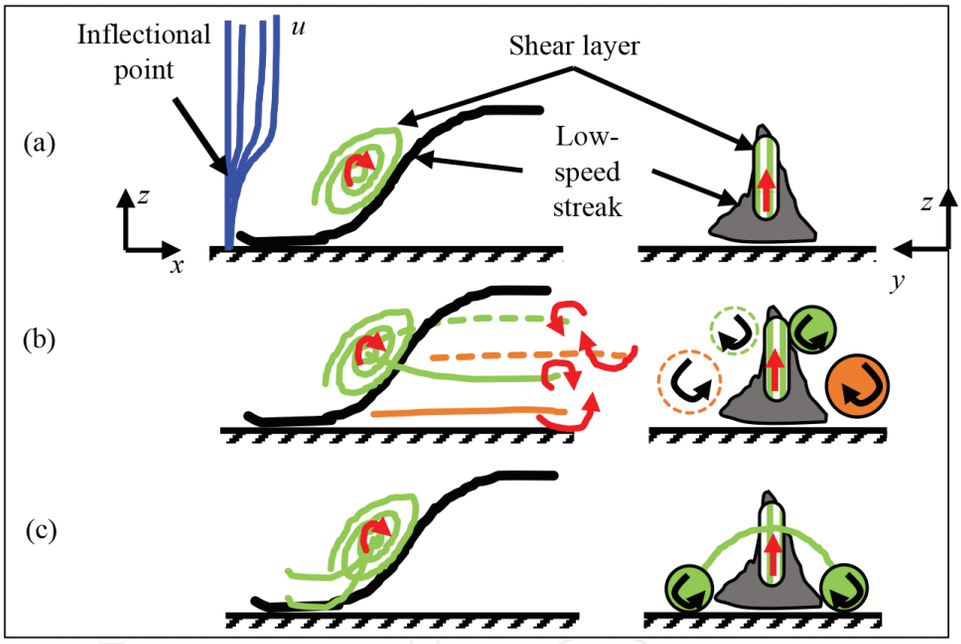

Figure 11. Generation of a streamwise vortex during the bursting process. (a) Lifted low-speed streak, (b) presence of the lifting streamwise vortex at one side of the streak, and (c) absence of the lifting vortex and generation of an arch vortex.

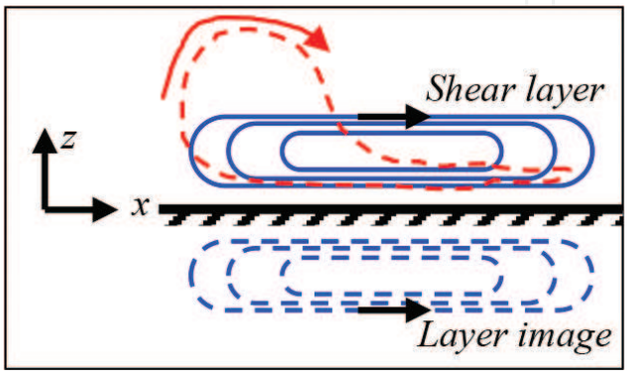

Figure 12. Roll-up of a streamwise shear layer by mutual induction with its image.

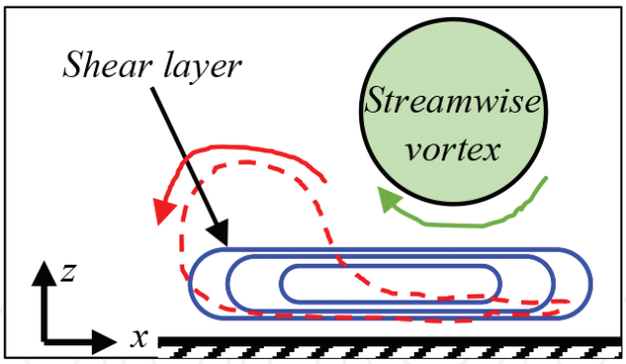

Figure 13. Roll-up of a streamwise shear layer by ejection from a parent vortex.

Either theory of the streamwise vortices implies that they are the main occupants of the viscous sublayer, whereas the outer layer is dominated by transverse vortices (heads of the hairpins). Bearing in mind their extended lengths compared to the spanwise (arch) vortices, the streamwise vortices are the main contributors to Reynolds stress in the sublayer [9, 27, 60, 66–71].

8. Turbulence sustenance by instability

In the foregoing discussion, the bursting process, and hence vortex generation, was almost totally undertaken by other coherent structures. This is termed the *parent-offspring* mechanism for turbulence production. On the contrary, a broad team of researchers designates a role in the vortex regeneration process to flow instabilities. The instabilities are supposed to take many forms and play different roles in turbulence generation [50, 72–74].

According to Swearingen and Blackwelder [75], instabilities motivate the generation of streamwise vortices and then trigger the generation of the hairpin vortices. Taylor-Görtler instabilities prevail near the wall due to streamline curvature, either as an inherent property of the TBL profile [73] or a result of the passage of a large-scale disturbance [36]. These can produce a system of streamwise vortices. The streamwise vortices in turn pump the fluid to build the low- and high-speed streaks. Consequently, two inflectional velocity profiles are formed ($U_{(z)}$ and $U_{(y)}$). From Rayleigh's criterion which has been upgraded by Fjørtoft's theorem, these inflectional profiles are inherently unstable [40, 55]. Thus, a secondary instability is generated which causes the streak lift-up, giving birth to new horseshoe vortices. Recall that the streak oscillations were interpreted by Kline et al. [37] as Kelvin-Helmholtz instabilities due to the growth and roll-up of the shear layer formed above the streak.

9. Large-scale motions (LSMs, vortex packets)

A vortex packet or large-scale motion is a bundle of hairpin vortices comprising 2–10 vortices aligned streamwise and traveling together. The inboard inductions of the hairpins against the mainstream combine together to form a relatively large region of uniform low momentum. The length of the packet ranges within 2–3δ. The recognition of vortex packets dates back to the early

hairpin vortex visualizations [76]. According to Smith [42], the arrangement of the hairpins in packets is a natural consequence of their production as groups (2–5 vortices) in the bursting process. Zhou et al. [14] conducted a DNS to study the mechanism of generation of vortex packets. The simulation started with a pair of counter-rotating streamwise vortices which evolved into a hairpin. If this primary hairpin is strong enough, its induced flow interacts with the mean flow or induced flow from another hairpin to deliver secondary, tertiary, and downstream vortices. This vortex spawning complies with the findings of Doligalski et al. [77]. The final tent-like shape of the packet is very similar to the early hypothesis of Head and Bandyopadhyay [76].

The primary vortex and its offspring flock together as a packet. Adrian and his team [21, 78] further extended their *vortex packet paradigm* through experimentally studying the vortex packet behavior in the outer layer. The inboard induction of the packet hairpins against the main stream causes the packet to travel at a speed slower than the mean flow ($\sim 0.8\, U_\infty$). As the hairpin ages, it expands in size and hence the induction is attenuated. Thus, the upstream parent hairpin moves faster than the downstream offspring; the packet stretches in the streamwise direction. Progressively, the overall induction of the packet hairpins is weakened. In addition, the hairpins move to higher faster fluid layers. Consequently, older packets move faster than younger packets and may overrun them. Packets can also merge with adjacent packets either streamwise or spanwise to form larger, stronger ones [79]. A vortex packet can extend to the edge of the boundary layer to form at least part of the turbulent bulges [3, 80]. Surprisingly, the description of the turbulent bulges introduced by Kovasznay et al. [81] agrees with that of the vortex packets. Moreover, Brown and Thomas [73] conducted correlation analysis across 75% of the TBL. They recognized large structures of length $2\,\delta$ and 18° inclination angle. From their PIV analysis, Ganapathisubramani et al. [82] confirmed the existence of the hairpin vortex packets. They could identify packets as long as $2\,\delta$. The packets hold more than 25% of Reynolds stress although occupying less than 4% of the total area. However, Ganapathisubramani et al. expected the packets to break down outside the logarithmic layer. While the angle of inclination of the hairpin vortex fluctuates around 45°, the packet as a whole leans against the wall at an angle of 10.5–13° [21, 78]. The LSMs are accompanied on either side with somehow shorter high-speed structures [13].

The vortex packet paradigm [21] assumes some kind of interaction between the large and small vortex packets. The larger packets move at higher speeds than the smaller ones such that they overtake them. As such, the smaller packets are liable to be enclosed in the uniform momentum zones of larger packets. As a consequence, the velocity vectors of the small scales undergo modulation by the larger ones. A modulating role for the large scales on the near-wall streaks was proven by Toh and Itano [83]. The modulation comprises the three velocity components [84] and extends to the frequency [85]. However, Hutchins [86] seizes the modulation to the near-wall region and interprets the similarity in amplitude between the scales outside it as a mere matter of preferential arrangement.

10. Very large scale motions (VLSMs, superstructures)

From their power spectral analysis of the streamwise velocity signal in channel and pipe flows, Jiménez [87] and Kim and Adrian [80] discovered a bimodal trend for the premultiplied spectrum. The two spectrum peaks correspond to wavelengths of 2–3 δ and 12–20 δ. The former was

attributed to vortex packets (or turbulent bulges) whereas the latter was attributed to a turbulence coherent structure that extends very long streamwise. It was therefore named the very large scale motion (VLSM) or superstructure. Kim and Adrian conjectured that hairpins align in groups to form long LSMs, and LSMs in turn align coherently to form superstructures, see **Figure 14**. This hierarchical structure has been proven by Baltzer et al. [88] and received approbation from other authors [79, 89]. Nevertheless, Bailey et al. [90] found a disparity between the transverse (azimuthal) scales of both LSMs and superstructures that suggests the latter to be formed either by alignment of the biggest LSMs or separately from flow instabilities. Moreover, Hwang and Cossu [91–93] found from large eddy simulations (LESs) that the superstructures self-sustain even when the small-scale structures in the buffer and logarithmic layers are artificially quenched.

Superstructures were recorded over the lower half of the turbulent boundary layer, including the logarithmic region [89]. The superstructures contribute 50% to the turbulent kinetic energy and more than 50% to the Reynolds shear stress [94, 95]. Dennis and Nickels [89] conducted experimental (3D PIV + Talyor's hypothesis) tests on boundary layer flow from which they estimated the length of superstructures to be limited to 7 δ. However, superstructures as large as 30 δ were found in pipe flow by DNS held by Lee and Sung [96] and by hotwire measurements held by Monty et al. [97]. The large difference between the two turbulent flows is caused by the free surface in case of TBL where entrainment occurs of large plumes from the free stream into the TBL. This entrainment breaks down the long coherent structures. Hutchins and Marusic [98] provided direct evidence of the superstructures in the logarithmic and lower wake regions of the turbulent boundary layer and atmospheric surface layer through velocity contours obtained from a rack of hotwires and sonic anemometers. Moreover, they found the superstructures to meander extremely along their length. The low-speed superstructures are usually twinned with high-speed structures of comparable lengths, probably induced by hairpin vortex legs [89]. The superstructure resembles an outer-layer counterpart of the low-speed streak [33]. The first is 12–20 δ long and 3–4 δ spanwise spaced, whereas the second is 1000 wall-units long and 100 wall-units spanwise spaced. Carlotti [99] differentiates between the two structures based on spectral analysis; the superstructures produce a "-1" power slope and the low-speed streaks produce a "-2" power slope.

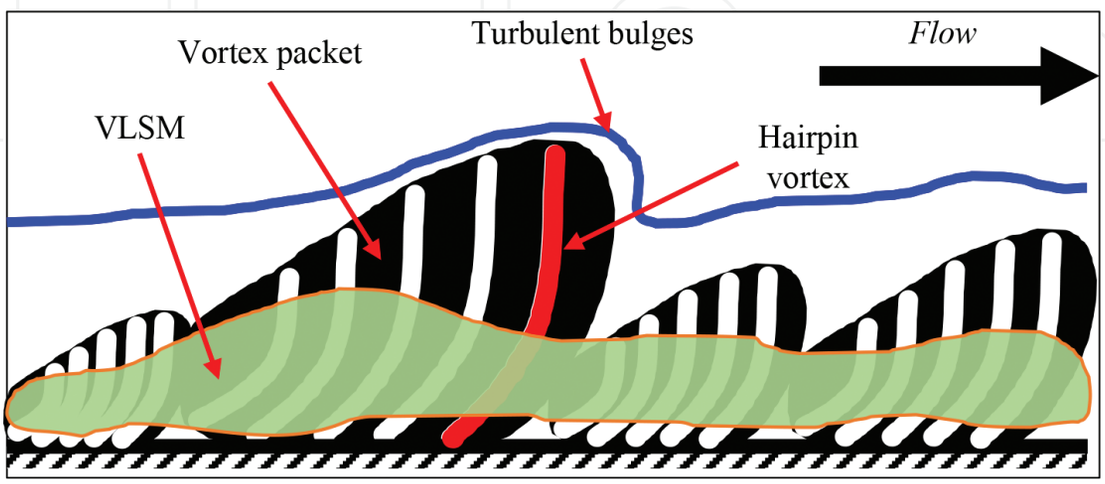

Figure 14. A VLSM turns out from agglomeration of several vortex packets aligned in the streamwise direction.

http://dx.doi.org/10.5772/intechopen.76854

The newly discovered coherent structures (LSM and VLSMs) have been used to develop the old attached eddy model of Townsend [7]. Perry and co-authors [15, 18] devised a model to predict turbulence statistics by applying the attached eddy hypotheses to *a forest of hairpin vortices* of sizes proportional to their height from the wall. The model has been further polished by Marusic [100] who found the vortex packet to best resemble the attached eddies and prescribe turbulence statistics. Exactly the same was deduced by Dennis and Nickels [13]. Del Álamo et al. [101] inferred that the logarithmic region is populated with two classes of clusters; small detached vortex packets and tall attached packets. Hwang and Cossu [91–93] displayed that the energy-containing motions at a given spanwise length scale can self-sustain themselves by extracting energy directly from the mean flow even with the absence of any larger or smaller structures. They found the sizes of these energy-containing motions to be proportional to their distances from the wall, which makes them good candidates to be Townsend's attached eddies. However, they anticipated each of these eddies to be composed of two elements, a long streaky structure and a vortical structure. In the sublayer, these are the low-speed streak and the quasi-streamwise vortices flanking it and in the logarithmic and wake layers, these are the superstructures and the vortex packets aligning along them.

11. Generation of mechanical coherent structures in the ABL

The outer layer flow has generally been neutralized in the discussion about coherent structure generation. It was assumed that the structures are pure products of surface-instability interactions. This *bottom-up* model is convincing at low Re_τ where the inner layer resembles a considerable portion of the whole boundary layer depth. Nevertheless, as Re_τ increases, the inner and outer scales separate. For instance, the atmospheric boundary layer (ABL) can extend in height up to 1000 m but its inner layer is no more than few centimeters. It follows that, the bottom-up mechanism presupposes that a vortex packet of 5-cm size is to enlarge persistently tens of meters within a high Re_τ turbulent flow field until reaching the turbulent/non-turbulent interface.

Many authors [16, 17, 38, 40, 54, 73, 102, 103] recorded that the structures within the outer layer can trigger the bursting process, *top-down* models. Based on the synchronization between the bursting process and the passage of turbulent bulges in the turbulent/non-turbulent interface, Blackwelder and coworkers [28, 104, 105] conjectured that either the bursting phenomenon controls the outer flow field by developing the large-scale bulges, or else the outer field drives the bursts. Falco [106] observed the bulges at the turbulent/non-turbulent interface. He found the bulges to encompass *typical eddies*. These are ring or hairpin eddies found in almost all turbulent flows; wakes, jets, grid-generated turbulence; turbulent boundary layers, etc. In their proposed Overall Production Module, Falco, Klewicki, and Pan [107] hypothesized the bursting process to be triggered by a typical eddy moving toward the wall. The typical eddy when passing over a pair of low-speed streaks provokes the generation of two spanwise vortices within the streak pair, a primary vortex and a pocket vortex. The pocket in between opens up by self-induction and a sweep stream is created. Secondary hairpin vortices form across each streak. They are then twisted and rotated back toward the wall into the center of the pocket. This model largely coincides with the observations of Haidari and Smith [108].

Jiménez and Pinelli [62] utilized the capabilities of DNS to isolate the different turbulence sustenance mechanisms. They found that, at the studied Re_τ, turbulence can feed solely on the inner-layer cycle without any perturbations from the outer layer. However, Jiménez and Pinelli believe that the outer-layer perturbations still can maintain turbulence, yet at a lower activity. Between the bottom-up and top-down supporters, a third group of researchers [55, 109, 110] reckons that both models do coexist all the time with the former prevailing at low Re_τ and the latter at high Re_τ. Hunt and Morrison [103] suggest an Re_τ of 10^4 as a limiting value between the dominance regimes of both models.

Lin et al. [111] conducted an LES for neutral ABL. They employed a conditional sampling technique to track the evolution of the coherent structures. They concluded that hairpin vortices can be spawned by interaction between the ejection stream and either the mean flow or a sweep stream, a fact that has been confirmed later via DNS [14] and PIV [21]. The most interesting result among theirs is that they confirmed the top-down mechanism to generate vortices; a sweep stream when it impinges onto the ground, generates an ejection stream. However, they found these ejection-induced streams not to correlate with the strong ejection streams dominating the surface layer. Hunt and Morrison [103] and coworkers [99, 112, 113] developed the top-down model originally proposed by Falco [106] to comply with the ABL. Their conjecture is that the large eddies impinge and scrape along the surface, forming an internal boundary layer. As such, streamwise vortices of lengths several times the boundary layer height are generated alongside the impinging eddy. When the generated vortices interact with others, they are lifted far upward. The theory further splits the atmospheric surface layer into two sublayers: the shear layer and the eddy surface layer. The shear dominates the spectra in the first by distorting turbulence isotropy, while in the second the statistics are dominated by the ground-blocking effect on the impinging eddies (normal velocity suppression). They supported their theory by observations from atmospheric flow and spectrum analysis from the near surface region. The layer division was proven by spectral analysis of field measurements undertaken by [114]. Likewise, McNaughton and Brunet [115] postulated that the outer-layer eddies overtake the superstructures and induce hairpin vortices in a similar fashion to the near-wall cycle proposed by Kline et al. [37].

12. Conclusion

The turbulent flow stays as one of the most difficult scientific problems man has encountered. Despite the great deal of advance in the field, the path from the mean flow to the random fluctuations is still controversial. The modern experimental and numerical techniques are either one-eyed or biased toward the flow conditions synthesized by the researchers. This chapter reviewed the accumulated knowledge of TCSs and unfolded and compared their different mechanisms of generation. The scope was confined to turbulent boundary layer flow and atmospheric flow.

In boundary layer flows, turbulence is sustained by two concurrent mechanisms, the bottom-up mechanism and the top-down mechanism. The former dominates in low-Reynolds number (FPBL) flows and the latter dominates in high-Reynolds number (atmospheric) flows. The bottom-up mechanism generates turbulence coherent structures by surface-instability interaction, whereas the top-down mechanism relies on large outer-layer structures to trigger the generation process. Both the FPBL flow and the atmospheric flow share common features and are occupied by similar

turbulence coherent structures, namely, the streamwise vortices, the low-speed streaks, the hairpin vortices, the vortex packets, and the superstructures. However, the large scale in atmospheric flow neutralizes the role of the low-speed streaks and streamwise vortices. Many conceptual and numerical models have been set forth to enhance our understanding of turbulent flows. The research is always aiming to achieve a model that can be implemented in numerical simulations or drag reduction applications. In the end, despite the vast knowledge of turbulent flow structure, turbulence continues to be an unsolved or not thoroughly understood phenomenon.

Author details

Zambri Harun[1]* and Eslam Reda Lotfy[1,2]

*Address all correspondence to: zambri@ukm.edu.my

1 Faculty of Engineering and Built Environment, Universiti Kebangsaan Malaysia, Selangor, Malaysia

2 Mechanical Engineering Department, Alexandria University, Alexandria, Egypt

References

[1] Theodorsen T. Mechanism of turbulence. In: Proceedings of the Second Midwestern Conference on Fluid Mechanics. Vol. 1719; 1952

[2] Head MR, Bandyopadhyay P. New aspects of turbulent boundary-layer structure. Journal of Fluid Mechanics. 1981;**107**:297-338

[3] Adrian RJ. Hairpin vortex organization in wall turbulence. Physics of Fluids. 2007;**19**:41301

[4] Brooke JW, Hanratty TJ. Origin of turbulence-producing eddies in a channel flow. Physics of Fluids A: Fluid Dynamics. 1993;**5**:1011-1022

[5] Townsend AA. The Structure of Turbulent Shear Flow. Cambridge, New York; Cambridge University Press; 1956

[6] Grant HL. The large eddies of turbulent motion. Journal of Fluid Mechanics. 1958;**4**: 149-190

[7] Townsend AA. The Structure of Turbulent Shear Flow. Cambridge, New York: Cambridge Univ Press; 1976. p. 438p

[8] Willmarth WW, Tu BJ. Structure of turbulence in the boundary layer near the wall. Physics of Fluids. 1967;**10**:S134-S137

[9] Guezennec YG, Piomelli U, Kim J. On the shape and dynamics of wall structures in turbulent channel flow. Physics of Fluids A: Fluid Dynamics. 1989;**1**:764-766

[10] Robinson SK. Coherent motions in the turbulent boundary layer. Annual Review of Fluid Mechanics. 1991;**23**:601-639

[11] Klewicki J. Connecting vortex regeneration with near-wall stress transport. In: 29th AIAA, Fluid Dynamics Conference; 1998. p. 2963

[12] Smith CR, Walker JDA. Turbulent wall-layer vortices. Fluid Mechanics and its Applications. 1995;**30**:235

[13] Dennis DJC, Nickels TB. Experimental measurement of large-scale three-dimensional structures in a turbulent boundary layer. Part 1. Vortex packets. Journal of Fluid Mechanics. 2011;**673**:180-217

[14] Zhou J, Adrian RJ, Balachandar S, Kendall TM. Mechanisms for generating coherent packets of hairpin vortices in channel flow. Journal of Fluid Mechanics. 1999;**387**:353-396

[15] Perry AE, Henbest S, Chong MS. A theoretical and experimental study of wall turbulence. Journal of Fluid Mechanics. 1986;**165**:163-199

[16] Praturi AK, Brodkey RS. A stereoscopic visual study of coherent structures in turbulent shear flow. Journal of Fluid Mechanics. 1978;**89**:251-272

[17] Smith CR. Visualization of turbulent boundary layer structure using a moving hydrogen bubble wire probe. In: Lehigh Workshop on Coherent Structure in Turbulent Boundary Layers; 1978. pp. 48-49

[18] Perry AE, Chong MS. On the mechanism of wall turbulence. Journal of Fluid Mechanics. 1982;**119**:173-217

[19] Lozano-Durán A, Jiménez J. Time-resolved evolution of coherent structures in turbulent channels: Characterization of eddies and cascades. Journal of Fluid Mechanics. 2014;**759**:432-471

[20] Brinkerhoff JR, Yaras MI. Numerical investigation of the generation and growth of coherent flow structures in a triggered turbulent spot. Journal of Fluid Mechanics. 2014;**759**:257-294

[21] Adrian RJ, Meinhart CD, Tomkins CD. Vortex organization in the outer region of the turbulent boundary layer. Journal of Fluid Mechanics. 2000;**422**:1-54

[22] Wallace JM, Eckelmann H, Brodkey RS. The wall region in turbulent shear flow. Journal of Fluid Mechanics. 1972;**54**:39-48

[23] Wilcox DC et al. Turbulence Modeling for CFD. Vol. 2. La Canada, CA: DCW Industries; 1998

[24] Corrsin S. Some current problems in turbulent shear flows. In: Symposium on Naval Hydrodynamics. Vol. 515; 1957

[25] Ferrell JK, Richardson FM, Beatty KO Jr. Dye displacement technique for velocity distribution measurements. Industrial and Engineering Chemistry. 1955;**47**:29-33

[26] Alfonsi G. Coherent structures of turbulence: Methods of eduction and results. Applied Mechanics Reviews. 2006;**59**:307-323

[27] Blackwelder RF, Eckelmann H. Streamwise vortices associated with the bursting phenomenon. Journal of Fluid Mechanics. 1979;**94**:577-594

[28] Blackwelder RF. The bursting process in turbulent boundary layers. In: Lehigh Workshop on Coherent Structure in Turbulent Boundary Layers; 1978, pp. 211-227

[29] Kim H, Kline SJ, Reynolds WC. The production of turbulence near a smooth wall in a turbulent boundary layer. Journal of Fluid Mechanics. 1971;**50**:133-160

[30] Schraub FA, Kline SJ. A Study of the Structure of the Turbulent Boundary Layer with and without Longitudinal Pressure Gradients. Stanford University; 1965

[31] Tu BJ, Willmarth WW. An Experimental Study of Turbulence near the Wall through Correlation Measurements in a Thick Turbulent Boundary Layer. Ann Arbor: Dept. Aerosp. Eng., University of Michigan; 1966. Technical Report No. 02920-3-T

[32] Smith CR, Metzler SP. The characteristics of low-speed streaks in the near-wall region of a turbulent boundary layer. Journal of Fluid Mechanics. 1983;**129**:27-54

[33] Pujals G, Garc'ia-Villalba M, Cossu C, Depardon S. A note on optimal transient growth in turbulent channel flows. Physics of Fluids. 2009;**21**:15109

[34] Del Álamo JC, Jimenez J. Linear energy amplification in turbulent channels. Journal of Fluid Mechanics. 2006;**559**:205-213

[35] Butler KM, Farrell BF. Optimal perturbations and streak spacing in wall-bounded turbulent shear flow. Physics of Fluids A: Fluid Dynamics. 1993;**5**:774-777

[36] Hamilton JM, Kim J, Waleffe F. Regeneration mechanisms of near-wall turbulence structures. Journal of Fluid Mechanics. 1995;**287**:317-348

[37] Kline SJ, Reynolds WC, Schraub FA, Runstadler PW. The structure of turbulent boundary layers. Journal of Fluid Mechanics. 1967;**30**:741-773

[38] Willmarth WW. Structure of turbulence in boundary layers. Advances in Applied Mechanics. 1975;**15**:159-254

[39] Corino ER, Brodkey RS. A visual investigation of the wall region in turbulent flow. Journal of Fluid Mechanics. 1969;**37**:1-30

[40] Grass AJ. Structural features of turbulent flow over smooth and rough boundaries. Journal of Fluid Mechanics. 1971;**50**:233-255

[41] Nakagawa H, Nezu I. Structure of space-time correlations of bursting phenomena in an open-channel flow. Journal of Fluid Mechanics. 1981;**104**:1-43

[42] Smith CR. A Synthesized Model of the Near-Wall Behavior in Turbulent Boundary Layers. Bethlehem Pennsylvania: Department of Mechanical Engineering and Mechanics, Lehigh University; 1984

[43] Black TJ. An analytical study of the measured wall pressure field under supersonic turbulent boundary layers. National Aeronautics and Space Administration. Washington D.C.; 1968

[44] Runstadler PW, Kline SJ, Reynolds WC. An experimental investigation of the flow structure of the turbulent boundary layer. Stanford University, California: 1963

[45] Harun Z, Monty JP, Mathis R, Marusic I. Pressure gradient effects on the large-scale structure of turbulent boundary layers. Journal of Fluid Mechanics. 2013;**715**:477-498

[46] Blackwelder RF, Kovasznay LSG. Large-scale motion of a turbulent boundary layer during relaminarization. Journal of Fluid Mechanics. 1972;**53**:61-83

[47] Cannon JN. Heat transfer from a fluid flowing inside a rotating cylinder [thesis]. Stanford University; 1965

[48] Halleen RM, Johnston JP. The Influence of Rotation on Flow in a Long Rectangular Channel: An Experimental Study. California: Stanford University, Thermosciences Division; 1967

[49] Eitel-Amor G, Örlü R, Schlatter P, Flores O. Hairpin vortices in turbulent boundary layers. Physics of Fluids. 2015;**27**:25108

[50] Schoppa W, Hussain F. Coherent structure generation in near-wall turbulence. Journal of Fluid Mechanics. 2002;**453**:57-108

[51] Jeong J, Hussain F. On the identification of a vortex. Journal of Fluid Mechanics. 1995;**285**: 69-94

[52] Schwartz SP. Investigation of vortical motions in the inner region of a turbulent boundary layer [thesis]; 1981

[53] Offen GR, Kline SJ. A proposed model of the bursting process in turbulent boundary layers. Journal of Fluid Mechanics. 1975;**70**:209-228

[54] Offen GR, Kline SJ. Combined dye-streak and hydrogen-bubble visual observations of a turbulent boundary layer. Journal of Fluid Mechanics. 1974;**62**:223-239

[55] Panton RL. Overview of the self-sustaining mechanisms of wall turbulence. Progress in Aerospace Science. 2001;**37**:341-383

[56] Dennis DJC. Coherent structures in wall-bounded turbulence. Anais da Academia Brasileira de Ciências. 2015;**87**:1161-1193

[57] Bernard PS, Thomas JM, Handler RA. Vortex dynamics and the production of Reynolds stress. Journal of Fluid Mechanics. 1993;**253**:385-419

[58] Miyake Y, Ushiro R, Morikawa T. The regeneration of quasi-streamwise vortices in the near-wall region. JSME International Journal Series B: Fluids and Thermal Engineering. 1997;**40**:257-264

[59] Zhang N, Lu L, Duan Z, Yuan X. Numerical simulation of quasi-streamwise hairpin-like vortex generation in turbulent boundary layer. Applied Mathematics and Mechanics. 2008;**29**:15-22

[60] Heist DK, Hanratty TJ, Na Y. Observations of the formation of streamwise vortices by rotation of arch vortices. Physics of Fluids. 2000;**12**:2965-2975

[61] Schoppa W, Hussain F. Genesis of longitudinal vortices in near-wall turbulence. Meccanica. 1998;**33**:489-501

[62] Jiménez J, Pinelli A. The autonomous cycle of near-wall turbulence. Journal of Fluid Mechanics. 1999;**389**:335-359

[63] Sendstad O. The near wall mechanics of three-dimensional turbulent boundary layers. Stanford University, California; 1992

[64] Jiménez J, Orlandi P. The rollup of a vortex layer near a wall. Journal of Fluid Mechanics. 1993;**248**:297-313

[65] Orlandi P. Vortex dipole rebound from a wall. Physics of Fluids A: Fluid Dynamics. 1990;**2**:1429-1436

[66] Kim J, Moin P, Moser R. Turbulence statistics in fully developed channel flow at low Reynolds number. Journal of Fluid Mechanics. 1987;**177**:133-166

[67] Bakewell HP Jr, Lumley JL. Viscous sublayer and adjacent wall region in turbulent pipe flow. Physics of Fluids. 1967;**10**:1880-1889

[68] Robinson SK. The kinematics of turbulent boundary layer structure. NASA STI/Recon Technical Report N. 1991;**91**:26465

[69] Clark JA, Markland E. Vortex structures in turbulent boundary layers. Aeronautical Journal. 1970;**74**:243-244

[70] Clark JA, Markland E. Flow visualization in free shear layers. Journal of the Hydraulics Division. 1973;**99**:1897-1913

[71] Cantwell BJ. Organized motion in turbulent flow. Annual Review of Fluid Mechanics. 1981;**13**:457-515

[72] Benney DJ. A non-linear theory for oscillations in a parallel flow. Journal of Fluid Mechanics. 1961;**10**:209-236

[73] Brown GL, Thomas ASW. Large structure in a turbulent boundary layer. Physics of Fluids. 1977;**20**:S243-S252

[74] Phillips WRC, Wu Z, Lumley JL. On the formation of longitudinal vortices in a turbulent boundary layer over wavy terrain. Journal of Fluid Mechanics. 1996;**326**:321-341

[75] Swearingen JD, Blackwelder RF. The growth and breakdown of streamwise vortices in the presence of a wall. Journal of Fluid Mechanics. 1987;**182**:255-290

[76] Head MR, Bandyopadhyay P. Combined flow visualization and hot wire measurements in turbulent boundary layers. In: Smith CR, Abbott, editors. Lehigh Workshop on Coherent Structure in Turbulent Boundary Layers; 1978. pp. 98-129

[77] Doligalski TL, Smith CR, Walker JDA. Vortex interactions with walls. Annual Review of Fluid Mechanics. 1994;**26**:573-616

[78] Christensen KT, Adrian RJ. Statistical evidence of hairpin vortex packets in wall turbulence. Journal of Fluid Mechanics. 2001;**431**:433-443

[79] Lee JH, Sung HJ. Very-large-scale motions in a turbulent boundary layer. Journal of Fluid Mechanics. 2011;**673**:80-120

[80] Kim KC, Adrian RJ. Very large-scale motion in the outer layer. Physics of Fluids. 1999;**11**:417-422

[81] Kovasznay LSG, Kibens V, Blackwelder RF. Large-scale motion in the intermittent region of a turbulent boundary layer. Journal of Fluid Mechanics. 1970;**41**:283-325

[82] Ganapathisubramani B, Longmire EK, Marusic I. Characteristics of vortex packets in turbulent boundary layers. Journal of Fluid Mechanics. 2003;**478**:35-46

[83] Toh S, Itano T. Interaction between a large-scale structure and near-wall structures in channel flow. Journal of Fluid Mechanics. 2005;**524**:249-262

[84] Talluru KM, Baidya R, Hutchins N, Marusic I. Amplitude modulation of all three velocity components in turbulent boundary layers. Journal of Fluid Mechanics. 2014;**746**:R1

[85] Baars WJ, Talluru KM, Hutchins N, Marusic I. Wavelet analysis of wall turbulence to study large-scale modulation of small scales. Experiments in Fluids. 2015;**56**:188

[86] Hutchins N. Large-scale structures in high Reynolds number wall-bounded turbulence. Progress in Turbulence V. Berlin: Springer; 2014, p. 75-83

[87] Jiménez J. The largest scales of turbulent wall flows. CTR Annual Research Briefs. 1998;**137**:54

[88] Baltzer JR, Adrian RJ, Wu X. Structural organization of large and very large scales in turbulent pipe flow simulation. Journal of Fluid Mechanics. 2013;**720**:236-279

[89] Dennis DJC, Nickels TB. Experimental measurement of large-scale three-dimensional structures in a turbulent boundary layer. Part 2. Long structures. Journal of Fluid Mechanics. 2011;**673**:218-244

[90] Bailey SCC, Hultmark M, Smits AJ, Schultz MP. Azimuthal structure of turbulence in high Reynolds number pipe flow. Journal of Fluid Mechanics. 2008;**615**:121-138

[91] Hwang Y, Cossu C. Self-sustained process at large scales in turbulent channel flow. Physical Review Letters. 2010;**105**:44505

[92] Cossu C, Hwang Y. Self-sustaining processes at all scales in wall-bounded turbulent shear flows. Philosophical Transactions of the Royal Society A. 2017;**375**:20160088

[93] Hwang Y. Statistical structure of self-sustaining attached eddies in turbulent channel flow. Journal of Fluid Mechanics. 2015;**767**:254-289

[94] Guala M, Hommema SE, Adrian RJ. Large-scale and very-large-scale motions in turbulent pipe flow. Journal of Fluid Mechanics. 2006;**554**:521-542

[95] Jimenez J, Del Alamo JC, Flores O. The large-scale dynamics of near-wall turbulence. Journal of Fluid Mechanics. 2004;**505**:179-199

[96] Lee JH, Sung HJ. Comparison of very-large-scale motions of turbulent pipe and boundary layer simulations. Physics of Fluids. 2013;**25**:45103

[97] Monty JP, Stewart JA, Williams RC, Chong MS. Large-scale features in turbulent pipe and channel flows. Journal of Fluid Mechanics. 2007;**589**:147-156

[98] Hutchins N, Marusic I. Evidence of very long meandering features in the logarithmic region of turbulent boundary layers. Journal of Fluid Mechanics. 2007;**579**:1-28

[99] Carlotti P. Two-point properties of atmospheric turbulence very close to the ground: Comparison of a high resolution LES with theoretical models. Boundary-Layer Meteorology. 2002;**104**:381-410

[100] Marusic I. On the role of large-scale structures in wall turbulence. Physics of Fluids. 2001;**13**:735-743

[101] Del Álamo JC, Jimenez J, Zandonade P, Moser RD. Self-similar vortex clusters in the turbulent logarithmic region. Journal of Fluid Mechanics. 2006;**561**:329-358

[102] Rao KN, Narasimha R, Narayanan MAB. The "bursting"phenomenon in a turbulent boundary layer. Journal of Fluid Mechanics. 1971;**48**:339-352

[103] Hunt JCR, Morrison JF. Eddy structure in turbulent boundary layers. European Journal of Mechanics - B/Fluids. 2000;**19**:673-694

[104] Blackwelder RF, Kaplan RE. On the wall structure of the turbulent boundary layer. Journal of Fluid Mechanics. 1976;**76**:89-112

[105] Blackwelder R. An experimental model for near-wall structure. In: 29th AIAA, Fluid Dynamics Conference; 1997. p. 2960

[106] Falco RE. Coherent motions in the outer region of turbulent boundary layers. Physics of Fluids. 1977;**20**:S124-S132

[107] Falco RE, Klewicki JC, Pan K. Production of turbulence in boundary layers and potential for modification of the near wall region. Structure of Turbulence and Drag Reduction. Berlin: Springer; 1990, p. 59-68

[108] Haidari AH, Smith CR. The generation and regeneration of single hairpin vortices. Journal of Fluid Mechanics. 1994;**277**:135-162

[109] Hutchins N, Chauhan K, Marusic I, Monty J, Klewicki J. Towards reconciling the large-scale structure of turbulent boundary layers in the atmosphere and laboratory. Boundary-Layer Meteorology. 2012;**145**:273-306

[110] Mathis R, Hutchins N, Marusic I. Large-scale amplitude modulation of the small-scale structures in turbulent boundary layers. Journal of Fluid Mechanics. 2009;**628**:311-337

[111] Lin C-L, McWilliams JC, Moeng C-H, Sullivan PP. Coherent structures and dynamics in a neutrally stratified planetary boundary layer flow. Physics of Fluids. 1996;**8**:2626-2639

[112] Högström U, Hunt JCR, Smedman A-S. Theory and measurements for turbulence spectra and variances in the atmospheric neutral surface layer. Boundary-Layer Meteorology. 2002;**103**:101-124

[113] Hunt JCR, Carlotti P. Statistical structure at the wall of the high Reynolds number turbulent boundary layer. Flow, Turbulence and Combustion. 2001;**66**:453-475

[114] Drobinski P, Carlotti P, Newsom RK, Banta RM, Foster RC, Redelsperger J-L. The structure of the near-neutral atmospheric surface layer. Journal of the Atmospheric Sciences. 2004;**61**:699-714

[115] McNaughton KG, Brunet Y. Townsend's hypothesis, coherent structures and Monin–Obukhov similarity. Boundary-Layer Meteorology. 2002;**102**:161-175

IntechOpen